Self-Assembly of Poly(ethylene glycol)-Poly(alkyl phosphonate) Terpolymers on Titanium Oxide Surfaces: Synthesis, Interface Characterization, Investigation of Nonfouling Properties...

ARTICLE *in* LANGMUIR · SEPTEMBER 2009

Impact Factor: 4.46 · DOI: 10.1021/la902110j · Source: PubMed

6 AUTHORS, INCLUDING:

Stefan Zürcher
ETH Zurich
50 PUBLICATIONS **1,473** CITATIONS
SEE PROFILE

Samuele G. P. Tosatti
ETH Zurich
60 PUBLICATIONS **2,359** CITATIONS
SEE PROFILE

Marcus Textor
ETH Zurich
333 PUBLICATIONS **13,999** CITATIONS
SEE PROFILE

Langmuir
Article
pubs.acs.org/Langmuir

Self-Assembly of Poly(ethylene glycol)−Poly(alkyl phosphonate) Terpolymers on Titanium Oxide Surfaces: Synthesis, Interface Characterization, Investigation of Nonfouling Properties, and Long-Term Stability

Vincent Zoulalian,[†,‡] Stefan Zürcher,[†] Samuele Tosatti,[†] Marcus Textor,[†] Sophie Monge,[‡] and Jean-Jacques Robin*[,‡]

[†]*Laboratory for Surface Science and Technology, Department of Materials, ETH Zurich, Wolfgang-Pauli-Strasse 10, CH-8093 Zurich, Switzerland, and* [‡]*Institut Charles Gerhardt Montpellier UMR5253 CNRS-UM2-ENSCM-UM1, Equipe Ingénierie et Architectures Macromoléculaires, Université Montpellier II cc1702, Place Eugène Bataillon, 34095 Montpellier Cedex 5, France*

Received June 12, 2009. Revised Manuscript Received July 29, 2009

This contribution deals with the self-assembling of a terpolymer on titanium oxide (TiO_2) surface. The polymer structure was obtained by polymerization of different methacrylates, i.e., alkyl-phosphonated, butyl and PEG methacrylate, in the presence of a chain transfer agent. The resulting PEG−poly(alkyl phosphonate) material, characterized mainly by SEC and NMR, self-organized at the interface of TiO_2. AR-XPS demonstrated the binding of phosphonate groups to TiO_2 substrate and the formation of a PEG−brush layer at the outermost part of the system. The stability of this terpolymer adlayer, after exposure to solutions of pH 2, 7.4, and 9 up to 3 weeks, was evaluated quantitatively by XPS and ellipsometry. We demonstrated an overall stability improvements of this coating against desorption in contact with aqueous solutions in comparison with reference self-assembly systems. Finally, the PEG−terpolymer adlayer proved to impart to TiO_2 substrate antifouling properties when exposed to full blood serum.

Introduction

The control of the physical and chemical properties of material surfaces is of prime importance when developing medical devices and biosensors. Indeed, when no specific surface treatment is applied on artificial materials, their direct exposure to biological fluids results generally in uncontrolled processes such as nonspecific adsorption of proteins followed by the formation of a biofilm.[1] Important modification systems based on spontaneous molecular assembly include self-assembled monolayers (SAMs) of alkanethiols on gold and alkanephosph(on)ates on metal oxides, respectively,[2−4] adlayers made from molecules containing biomimetic anchorage chemistry (e.g., dihydroxyphenylalanin (DOPA) derived from mussel adhesive proteins or cyanobacteria chelators),[5,6] and polyelectrolyte-grafted polymer interfaces.[7,8] They have been extensively investigated and fine-tuned to incorporate specific chemical structures and/or functional groups[9] with the aim of eliciting specific responses at surfaces of materials in contact with biological environment,[6,10−12] especially the elimination of nonspecific adsorption of proteins.[8,13,14]

To prevent unspecific biomolecular adsorption (e.g., of proteins) on artificial materials, a common method consists in immobilizing on their surfaces nonfouling or protein-resistant polymers,[15−18] such as poly(ethylene glycol) (PEG).[19−22] The latter is able to prevent the adhesion of proteins once immobilized as a dense brush on surfaces.[12,13,23−25] High degree of hydration (more than 80% in weight), steric repulsion by the polymer chains, and ability to screen interfacial charges were believed to be the main reasons to explain its successful nonfouling property. Among the possibilities to immobilize PEG−brush structures on

*Corresponding author: Tel 33-4-67-14-41-57, Fax 33-4-67-14-40-28, e-mail Jean-Jacques.Robin@univ-montp2.fr.

(1) Wahlgren, M.; Arnebrant, T. *Trends Biotechnol.* **1991**, *9*, 201–208.
(2) Ulman, A. *Chem. Rev.* **1996**, *96*, 1533–1554.
(3) Spori, D. M.; Venkataraman, N. V.; Tosatti, S. G. P.; Durmaz, F.; Spencer, N. D.; Zurcher, S. *Langmuir* **2007**, *23*, 8053–8060.
(4) Tosatti, S.; Michel, R.; Textor, M.; Spencer, N. D. *Langmuir* **2002**, *18*, 3537–3548.
(5) Lee, H.; Dellatore, S. M.; Miller, W. M.; Messersmith, P. B. *Science* **2007**, *318*, 426–430.
(6) Zurcher, S.; Wackerlin, D.; Bethuel, Y.; Malisova, B.; Textor, M.; Tosatti, S.; Gademann, K. *J. Am. Chem. Soc.* **2006**, *128*, 1064–1065.
(7) Kenausis, G. L.; Voros, J.; Elbert, D. L.; Huang, N. P.; Hofer, R.; Ruiz-Taylor, L.; Textor, M.; Hubbell, J. A.; Spencer, N. D. *J. Phys. Chem. B* **2000**, *104*, 3298–3309.
(8) Wagner, V. E.; Koberstein, J. T.; Bryers, J. D. *Biomaterials* **2004**, *25*, 2247–2263.
(9) Krishnan, S.; Weinman, C. J.; Ober, C. K. *J. Mater. Chem.* **2008**, *18*, 3405–3413.
(10) Gnauck, M.; Jaehne, E.; Blaettler, T.; Tosatti, S.; Textor, M.; Adler, H. J. P. *Langmuir* **2007**, *23*, 377–381.
(11) Rundqvist, J.; Hoh, J. H.; Haviland, D. B. *Langmuir* **2005**, *21*, 2981–2987.
(12) Feller, L. M.; Cerritelli, S.; Textor, M.; Hubbell, J. A.; Tosatti, S. G. P. *Macromolecules* **2005**, *38*, 10503–10510.
(13) Li, L. Y.; Chen, S. F.; Zheng, J.; Ratner, B. D.; Jiang, S. Y. *J. Phys. Chem. B* **2005**, *109*, 2934–2941.
(14) Dalsin, J. L.; Lin, L. J.; Tosatti, S.; Voros, J.; Textor, M.; Messersmith, P. B. *Langmuir* **2005**, *21*, 640–646.
(15) Chang, Y.; Chen, S. F.; Zhang, Z.; Jiang, S. Y. *Langmuir* **2006**, *22*, 2222–2226.
(16) Chen, S. F.; Liu, L. Y.; Jiang, S. Y. *Langmuir* **2006**, *22*, 2418–2421.
(17) Kane, R. S.; Deschatelets, P.; Whitesides, G. M. *Langmuir* **2003**, *19*, 2388–2391.
(18) Feng, W.; Brash, J. L.; Zhu, S. P. *Biomaterials* **2006**, *27*, 847–855.
(19) Dalsin, J. L.; Messersmith, P. B. *Mater. Today* **2005**, *8*, 38–46.
(20) Bretagnol, F.; Lejeune, M.; Papadopoulou-Bouraoui, A.; Hasiwa, M.; Rauscher, H.; Ceccone, G.; Colpo, P.; Rossi, F. *Acta Biomater.* **2006**, *2*, 165–172.
(21) Harris, J. M. *Poly(ethylene glycol) Chemistry: Biotechnical and Biomedical Applications*; Plenum Press: New York, 1992.
(22) Krsko, P.; Libera, M. *Mater. Today* **2005**, *8*, 36–44.
(23) Boulmedais, F.; Frisch, B.; Etienne, O.; Lavalle, P.; Picart, C.; Ogier, J.; Voegel, J. C.; Schaaf, P.; Egles, C. *Biomaterials* **2004**, *25*, 2003–2011.
(24) Satomi, T.; Nagasaki, Y.; Kobayashi, H.; Otsuka, H.; Kataoka, K. *Langmuir* **2007**, *23*, 6698–6703.
(25) Pasche, S.; De Paul, S. M.; Voros, J.; Spencer, N. D.; Textor, M. *Langmuir* **2003**, *19*, 9216–9225.

surfaces, one standard method is by means of a "grafting to" strategy, i.e., by the formation of an organic interface by chemisorption or physisorption of molecules presenting already grafted PEG chains as for instance PEGylated SAMs,[10,13,26] DOPA-functionalized molecules with PEG chains,[6,14] and polyelectrolyte−grafted PEG copolymers.[8,25,27] There is still a substantial interest to develop novel surface systems that can be cost effectively produced under mild conditions (room temperature, neutral or near neutral pH)[28,29] while achieving the following properties:[30] long-term robustness under a variety of relevant conditions (e.g., low/high pH and high ionic strength) and formation of a dense interfacial (brush) layer of hydrophilic polymer chains, e.g., with poly(ethylene glycol) (PEG), imparting nonfouling properties to the material or device surface.

Limitations of currently available self-assembly systems include potential loss of adlayer adhesion under physiological or other conditions (pH and ionic strength) by molecular desorption either due to chemical modification such as oxidation of anchoring groups in SAMs of thiols and DOPA systems[31−33] or due to weak electrostatic interactions in the case of polyelectrolyte−grafted polymer adlayers.[34−37] A second reason, specific to ordered, close-packed SAM systems, is the loss of order and stability when functionalized with bulky terminal groups[38−41] such as PEG chains. Finally, the requirement of adsorption conditions different from physiological conditions (e.g., pH, high ionic strength, temperature) to favor binding of PEG systems at high surface density ("cloud-point grafting")[5,6,14,42] may not be compatible with biological functionalities.

We have recently reported[43] the successful development of a new polymer class for the production, by self-assembly, of nonfouling surfaces on TiO_2-coated substrates (mimicking the surface properties of the important biomaterial titanium).[44] The polymer consisted of a terpolymer structure presenting on a backbone both grafted PEG chains and alkyl side chains carrying phosphonate end groups. Thanks to multivalent binding of the oligo-phosphonate polymer, the coated TiO_2 surfaces proved to have favorable stability up to 3 weeks when tested in solutions of different pH and in comparison to two reference systems, dodecylphosphonate ($DDPO_4$) SAMs[4] and poly(L-lysine)-*grafted*-poly(ethylene glycol) (PLL-*g*-PEG) on the same substrate.[25]

In this present work, we reported on further investigations allowing a better characterization of the system studied. We have quantitatively proved the antifouling properties of the PEG−poly(alkyl phosphonate) terpolymer assembled on TiO_2-coated surfaces by OWLS measurements and characterizing its interface organization using XPS and angle-resolved XPS (AR-XPS). We also investigated the longer term stability of this terpolymer surface after exposure to solutions of pH 2, 7.4, and 9 and a salt buffer with a pH = 7.4 up to 3 weeks, by XPS and ellipsometry. Such a series of experiments showed that nonstandard degradation processes such as desorption or hydrolysis reaction affected the adlayer stability but rather unusual mechanisms: PEG autoxidation and photoreactions initiated by the substrate. In view of photochemical reactions related to photocatalytic activities of the TiO_2 surface, tests were also performed with samples exposed to light or stored in the dark and compared to another type of substrate material (Nb_2O_5). Dodecylphosphate SAMs[4] and PLL-*g*-PEG assembled layers on TiO_2 surfaces[25] were used as reference.

Experimental Part

Characterization Techniques. ^{1}H NMR spectra (δ, ppm) were performed at room temperature on a 250 MHz Bruker spectrometer in deuterated $CDCl_3$ and CD_3OD as solvents with tetramethylsilane as an internal standard. Polymerizations were carried out using standard Schlenk techniques under an inert atmosphere of nitrogen. Size exclusion chromatography (SEC) measurements were run on a "GPC 220, Polymer Laboratories LTD" equipped with a triple detection system and the following conditions of analysis were used: dimethylformamide (DMF) as eluent with a flow rate of 1 mL/min, a DMF/LiBr mixture to dissolve the polymer, and a column temperature of 80 °C. Data were evaluated based on a universal calibration performed with polystyrene references. To support the SEC results about the terpolymer molecular weights, elemental analyses were performed to quantify the phosphorus (ICP-AES: inductive coupled plasma−atomic emission spectroscopy) and sulfur traces (LECO CHN-932: infrared detection from SO_2 gases produced by oxygen combustion).

After assembly and stability tests, the resulting terpolymer adlayers were characterized by their thicknesses evaluated by variable angle spectroscopic ellipsometry (VASE) and complemented by their elemental and component surface compositions with X-ray photoelectron spectroscopy (XPS). Depth-dependent information (along the z direction) on the organization of the adsorbed terpolymer molecules was obtained by performing angle resolved-XPS (AR-XPS) measurements.

Ellipsometric data were obtained with a variable angle spectroscopic M-2000F ellipsometer (LOT Oriel GmbH, Darmstadt, Germany) instrument. The measurements were conducted in the spectral range of 370−1000 nm at three different angles of incidence (65°, 70°, and 75°) and fitted using WVASE32 analysis software. For processing the results of the terpolymer-coated substrates, a multilayer model was designed. The reference substrate before metal oxide sputter-coating consisted of a 0.5 mm thick silicon wafer coated with a silicon oxide layer of 2.3 nm. Subsequently, by using the ellipsometric equations[45] and a Cauchy's model for the refractive indices of the metal oxide sputter-coated layers and the polymer layers,[45] thicknesses were evaluated. Finally, percent remaining adlayer thickness values were always calculated for data interpretation by referring to the initial adlayer thickness measured right after assembly.

(26) Vanderah, D. J.; Valincius, G.; Meuse, C. W. *Langmuir* **2002**, *18*, 4674–4680.
(27) Malmsten, M.; Emoto, K.; Van Alstine, J. M. *J. Colloid Interface Sci.* **1998**, *202*, 507–517.
(28) Ladd, J.; Boozer, C.; Yu, Q. M.; Chen, S. F.; Homola, J.; Jiang, S. *Langmuir* **2004**, *20*, 8090–8095.
(29) Huang, N. P.; Voros, J.; De Paul, S. M.; Textor, M.; Spencer, N. D. *Langmuir* **2002**, *18*, 220–230.
(30) Blattler, T. M.; Pasche, S.; Textor, M.; Griesser, H. J. *Langmuir* **2006**, *22*, 5760–5769.
(31) Flynn, N. T.; Tran, T. N. T.; Cima, M. J.; Langer, R. *Langmuir* **2003**, *19*, 10909–10915.
(32) Roosjen, A.; de Vries, J.; van der Mei, H. C.; Norde, W.; Busscher, H. J. *J. Biomed. Mater. Res., Part B* **2005**, *73B*, 347–354.
(33) Guvendiren, M.; Messersmith, P. B.; Shull, K. R. *Biomacromolecules* **2008**, *9*, 122–128.
(34) Burke, S. E.; Barrett, C. J. *Langmuir* **2003**, *19*, 3297–3303.
(35) Menchaca, J.-L.; Jachimska, B.; Cuisinier, F.; Perez, E. *Colloids Surf., A* **2003**, *222*, 185–194.
(36) Kharlampieva, E.; Sukhishvili, S. A. *Langmuir* **2003**, *19*, 1235–1243.
(37) Farhat, T. R.; Schlenoff, J. B. *Langmuir* **2001**, *17*, 1184–1192.
(38) Dannenberger, O.; Weiss, K.; Himmel, H. J.; Jager, B.; Buck, M.; Woll, C. *Thin Solid Films* **1997**, *307*, 183–191.
(39) Sushko, M. L.; Shluger, A. L. *J. Phys. Chem. B* **2007**, *111*, 4019–4025.
(40) Tsai, M. Y.; Lin, J. C. *J. Biomed. Mater. Res.* **2001**, *55*, 554–565.
(41) Zwahlen, M.; Tosatti, S.; Textor, M.; Hahner, G. *Langmuir* **2002**, *18*, 3957–3962.
(42) Rodriguez, R.; Blesa, M. A.; Regazzoni, A. E. *J. Colloid Interface Sci.* **1996**, *177*, 122–131.
(43) Zoulalian, V.; Monge, S.; Zurcher, S.; Textor, M.; Robin, J. J.; Tosatti, S. *J. Phys. Chem. B* **2006**, *110*, 25603–25605.
(44) Brunette, D. M. *Titanium in Medicine: Material Science, Surface Science, Engineering, Biological Responses, and Medical Applications*; Springer: Berlin, 2001.
(45) Tompkins, H. G.; McGahan, W. A. *Spectroscopic Ellipsometry and Reflectometry: A User's Guide*; Wiley: New York, 1999.

Table 1. XPS Curve-Fitting Parameters Used To Model the C 1s Components of the Terpolymer Adlayer Adsorbed on TiO_2

C 1s components	binding energy difference (eV)	references	fwhm (eV)	intensity (*I*) constraints
C−C	reference (284.9)	4, 7, 47−49	1.6−1.7	free
C−**C**−O−C=O	+1.9 ± 0.15	4, 7, 47−49	1.6−1.7	$1 \times I_{(O-C=O)}$
O−**C**=O	+4.0 ± 0.15	4, 7, 47−49	1.6−1.7	free
C−C=O	+0.65 ± 0.1	4, 7, 47−49	1.6−1.7	$1 \times I_{(O-C=O)}$
C−**C**−O	+1.7 ± 0.15	4, 7, 47−49	1.6−1.7	free
C−P	+1.45 ± 0.15	4, 7, 47−49	1.6−1.7	$I_{(O-C=O)}/10$

Table 2. XPS Fitting Parameters Used To Model the O 1s Components of the Terpolymer Adlayer Adsorbed on TiO_2

O 1s components	binding energy difference (eV)	references	fwhm (eV)	intensity (*I*) constraints
Ti−**O**	reference (530.0)	4, 7, 47−49	free	free
Ti−**O**−H	+1.6 ± 0.15	4, 7, 47−49	Ti−**O** value	free
C−**O**−C=O	+3.6 ± 0.15	4, 7, 47−49	1.6−1.7	free
O=C	+2.5 ± 0.15	4, 7, 47−49	1.6−1.7	$1 \times I_{(C-O-C=O)}$
C−**O**−C/P−**O**−H	+2.7 ± 0.15	4, 7, 47−49	1.6−1.7	free
P−**O**−Ti/**O**=P	+1.3 ± 0.15	4, 7, 47−49	1.6−1.7	$I_{(C-O-C=O)}/10$

XPS spectra were recorded at a 90° emission angle with a SAGE 100 instrument (Specs, Berlin, Germany) at a pressure below 4×10^{-8} mbar using nonmonochromatized Al Kα radiation at 320 W (13 kV) and an electron-energy analyzer pass energy of 50 eV for low-resolution survey and of 14 eV for high-resolution element detail scans. The analyzed area was 6 mm^2, giving therefore a lateral averaged chemical composition. AR-XPS measurements were acquired at a pressure below 10^{-9} mbar on a VG Thetaprobe spectrometer equipped with a concentric hemispherical analyzer and using a monochromatic Al Kα source at 350 W with a spot size of 300 μm. Pass energies used were 250 eV for survey and 100 eV for detailed scans. The two-dimensional detector is collecting the electrons, which are discriminated for signal intensities in both photoelectron energy and photoemission angle. Twelve angles equally spaced by 5° and varying from 25.5° to 80.5° in respect to the surface normal were acquired. The program CasaXPS (Version 2.2.24) was used for data processing. With the SAGE XPS data, the elemental and component surface compositions were determined by a semiquantitative evaluation assuming a homogeneous perpendicular distribution in the overlayer (layers A−C of the model presented in Scheme 1). The measured intensities were corrected for their corresponding photoionization cross-section values (Scofield's sensitivity factors).[46] The experimental component analysis of the C 1s and O 1s signals was performed based on the assignments in Tables 1 and 2 determined by an iterative peak fitting starting from referenced values of component binding energies, full width at half-maximum (fwhm), and Gaussian to Lorentzian ratio reported in the literature.[4,7,47−49] All binding energies of the different components were referenced to the **C**−C aliphatic peak for C 1s detail spectrum (Table 1) and Ti−**O** peak for O 1s detail spectrum (Table 2). The full width at half-maximum (fwhm) was maintained between 1.6 and 1.8 for all elements and transitions using the sum of 40% Gaussian and 60% Lorentzian function. During this processing, the relative ratio between C−C−**C**−O−C=O, O−**C**=O, **C**−C=O, and **C**−P components and between **O**=C, **O**−C=O, and **O**=P/P−**O**−Ti contributions were constrained according to the known bulk polymer structure obtained by ^{1}H NMR (Tables 1 and 2). From evaluated XPS data, percent remaining atomic and component ratios were calculated for data interpretation by referring to the initial value obtained for the terpolymer adlayer right after assembly. AR-XPS data were processed for each angle using the binding energies and intensity constraints determined previously from the SAGE data (Tables 1 and 2). The fwhm was constrained differently, between 1.3 and 1.4 for C 1s components and between 1.4 and 1.5 for O 1s components, due to the higher resolution obtained with the monochromatic X-rays of this system, and the Gaussian−Lorentzian ratio was fixed to 30%. Afterward, only ratios of peak areas measured at the same angle were used for data interpretation. Moreover, they were always normalized for comparison by the highest ratio of the same components (peak areas also obtained at the same angle) within the same series of AR-XPS measurements.

Scheme 1. Model for the Monomolecular Organization of the PEG−Poly(alkyl phosphonate) Terpolymer on a TiO_2 Surface in a Four-Layer (A to D) System as a Basis for the Interpretation of the Angle-Dependent XPS Studies

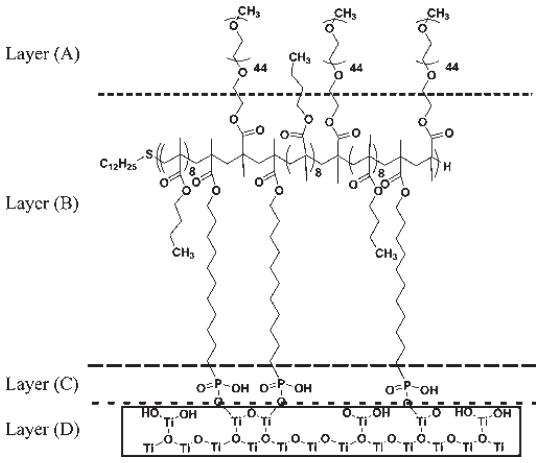

The resistance of the terpolymer interface against the adsorption of proteins under biological conditions (pH = 7.4 and 160 mM ionic strength) was measured using optical waveguide lightmode spectroscopy (OWLS). This technique allows calculating "dried" adsorbed masses in the vicinity of surfaces from the changes in refractive indices upon adsorption of molecules from solution. Changes are monitored by the grating-induced incoupling of a laser light into a waveguiding substrate, generating an evanescent field probing molecule uptake.[50] Adsorbed mass of proteins was calculated from the resulting thickness and refractive index of the new adlayer on the waveguide according to the de Feijter's formula[51] and the referenced dn/dc value of 0.182 cm^3/g.[25] The sensitivity limit of OWLS is typically 1−2 ng/cm.[2,50] Protein adhesion test was studied in situ, using a

(46) Scofield, J. H. *J. Electron Spectrosc. Relat. Phenom.* **1976**, *8*, 129–137.
(47) Huang, N. P.; Michel, R.; Voros, J.; Textor, M.; Hofer, R.; Rossi, A.; Elbert, D. L.; Hubbell, J. A.; Spencer, N. D. *Langmuir* **2001**, *17*, 489–498.
(48) Crist, B. V. *Polymers and Polymers Damaged by X-rays*; Wiley: Chichester, 2000.
(49) Moulder, J. F.; Chastain, J. *Handbook of X-ray Photoelectron Spectroscopy: A Reference Book of Standard Spectra for Identification and Interpretation of XPS Data*; Physical Electronics Division, Perkin-Elmer Corp.: Eden Prairie, MN, 1992.
(50) Voros, J.; Ramsden, J. J.; Csucs, G.; Szendro, I.; De Paul, S. M.; Textor, M.; Spencer, N. D. *Biomaterials* **2002**, *23*, 3699–3710.
(51) Defeijter, J. A.; Benjamins, J.; Veer, F. A. *Biopolymers* **1978**, *17*, 1759–1772.

flow cell with a volume of 16 mL. A TiO_2-coated waveguide, which has been ex situ coated with the terpolymer adlayer, was assembled in the OWLS flow cell. The system was equilibrated by immersion in 160 mM HEPES buffer (10 mM 4-(2-hydroxyethyl)piperazine-1-ethanesulfonic acid and 150 mM sodium chloride aqueous solution with pH adjusted to 7.4) for 4 h in order to condition the polymer molecules in biological solutions. Afterward, the antifouling capability of the terpolymer-coated OWLS chip was tested by exposure to full human serum (Control Serum N, Roche Diagnostics, Switzerland) for 15 min, followed by several rinses with HEPES buffer.

Synthesis and Bulk Characterization of Terpolymer Molecules. The synthesis protocol with the references of the reactants, their initial molar ratios, the terpolymer purification, and the procedure of ratio calculation with ^{1}H NMR have been previously reported.[43] The poly(phosphonate) terpolymer was synthesized by free-radical chain-transfer polymerization of dimethyl-11-methacryloyloxyundecyl phosphonates (C_{11})[52] with poly(ethylene glycol)methyl ether methacrylate (PEG) (molecular weight of 2000 g/mol) and *n*-butyl methacrylate (BMA). The aimed and characterized ratio of polymerized monomers was 1 to 1 to 8, respectively, with a degree of polymerization (DP_n) of about 30 monomers (Scheme 1).

In a typical experiment 1.392 g of dimethyl-(11-methacryloyloxyundecyl)phosphonate monomer (C_{11}) (4 mmol), 4 g (28 mmol) of freshly distilled *n*-butyl methacrylate monomer (BMA), 8.24 g (3.96 mmol) of carefully dried poly(ethylene glycol)methyl ether methacrylate (PEG), and 0.303 g (1.5 mmol) of 1-dodecanethiol were dissolved in acetonitrile (360 mL). The mixture was carefully degassed and saturated with nitrogen at room temperature. Benzoyl peroxide (0.087 g, 0.36 mmol into 10 mL of acetonitirile) was added at 85 °C. Polymerization occurred for 16 h under reflux. Subsequently, the solvent was evaporated and the polymer precipitated into *n*-pentane. The diester polymer was thus dissolved into dichloromethane (50 mL), and the reaction mixture was carefully degassed and saturated under an atmosphere of argon. 0.5 mL (3.8 mmol) of bromotrimethylsilane was added. At the end of the reaction, the solvent was evaporated and the remaining silanized intermediate was immediately dissolved in a methanol solution of NaOH (25.7 mg, 0.64 mmol, dissolved into 50 mL of methanol). The mixture was stirred for an additional 16 h. After evaporation of the solvent, the polymer was twice purified by precipitation into acetone to afford a white powder (0.68 g, yield 33.11%).

The molecular weights and the polydispersity of the synthesized terpolymers were determined only by analysis of the dimethyl phosphonic acid ester[43] due to the high probability of damages of chromatography columns with compounds containing free-phosphonic acid functions. SEC measurements were performed of freeze-dried samples previously dialyzed. The optimal conditions of dialysis—2 days against $\{Na_2HPO_4/KH_2PO_4\}$(4/1 w/w, 1.15 g/L) buffer with a 12−13 000 g/mol molecular weight cutoff membrane (Spectra-Por, Spectrum Laboratories, Inc.) followed by 2 days against ultrapure water—were determined after an optimization procedure and subsequently transposed to purify as well the final terpolymer compound with free phosphonates.[43] By considering eq 1 giving access to the number of repeating primary sequences of monomers whose composition was preliminary characterized with ^{1}H NMR (1/1/8 in C_{11}/PEG/BMA), the DP_n of the polymer backbone can be calculated and consequently the average molecular weight.

Assembly, Stability Tests, Protein Adsorption, and Surface Characterizations of Terpolymer Adlayer. Both 20 nm thick films of TiO_2 and 15 nm thick films of Nb_2O_5 were sputter-coated on silicon wafers ⟨110⟩ (WaferNet GmbH, Eching, Germany) using reactive magnetron sputtering (PSI, Villigen, Switzerland) to produce substrates for the terpolymer assemblies. Before adlayer formation, surfaces were sonicated twice in 2-propanol for 10 min, dried with N_2 (5.0), and UV-cleaned for 30 min (Boekel UV clean model 135500).

Spontaneously adsorbed terpolymer adlayers on previous cleaned surfaces were obtained by immersion of the chips for 16 h in a 0.5 mg/mL terpolymer aqueous solution prepared with ultrapure water from a Milli-Q system. Then the samples were rinsed with ultrapure water and dried with N_2 before surface characterizations and stability experiments.

Right after the fresh assembly of terpolymer molecules on substrates, stability of the resulting adlayers were tested by immersion in different aqueous solutions at room temperature and storage of the samples in γ-sterilized polystyrene cell-plate boxes (TPP, test plates, 92024), filled with acidic (HCl solution with a pH = 2), basic (NaOH solution with a pH = 9), or 160 mM HEPES buffer (10 mM 4-(2-hydroxyethyl) piperazine-1-ethanesulfonic acid and 150 mM sodium chloride aqueous solution with pH adjusted to 7.4) test solutions. When needed to protect the samples to daylight, an aluminum foil was wrapped around the cell-plate boxes. The time of immersion was varied between 4 h, 1 week, and 3 weeks. At the end of test periods, the samples were rinsed with ultrapure water and dried with N_2 prior to their characterizations of thickness (VASE) and surface composition (XPS) for the detection of polymer interface modifications.

The nonfouling property imparted by the terpolymer interfaces to substrates after stability experiments (i.e., acid, basic, and HEPES electrolyte exposures) was evaluated after the following protocol: exposure for 15 min to full human serum solution, followed by careful rinses with HEPES buffer and ultrapure water and drying with N_2. Adsorbed proteins were characterized by XPS measurements, by evaluating the presence of a nitrogen signal, which is specific for the proteins and not for the terpolymer structure (Scheme 1).[53]

Results and Discussion

Polymer Molecular Weight and Polydispersity. SEC measurements referenced to universal polystyrene calibration showed a monomodal peak corresponding to the terpolymer sample and a residual peak appearing at the highest retention time. The latter was attributed after verification with a control SEC measurement to residual PEG monomer remaining after purification steps. This assignment was supported by ^{1}H NMR as weak signals specific to unreacted PEG acrylate at characteristic chemical shifts ($\delta \approx 4.3$ ppm: $-CO-O-CH_2-CH_2$ $\delta \approx 5.5$ and 6.1 ppm: $CH_2{=}C-$). The SEC data obtained from the protected terpolymer sample dialyzed against $\{Na_2HPO_4/KH_2PO_4\}$(4/1 w/w, 1.15 g/L) buffer in a 12−13 000 g/mol molecular weight cutoff membrane can be used to judge the molecular weight, M_w, as 15 135 g/mol, which is in good agreement with the M_w resulting from the calculation of a polymer with 30 monomers (DP_n) with the ratios evaluated with ^{1}H NMR (ratio of C_{11}/PEG/BMA of 1 to 1 ± 1 to 8 ± 2)[43] of around 10 894 ± 850 g/mol. The small difference results not only from the residual PEG monomers but also from the polystyrene standards applied in SEC evaluation. Indeed, polystyrene does not present the same hydrodynamic volumes in DMF than the brushlike terpolymer, rendering the calibration slightly out of fit. Finally, the polydispersity index (I_p) of 2.99 is in agreement with the standard values usually obtained for chain-transfer free-radical polymerization.[54,55]

Based on the elemental analysis, $P = 0.6 \pm 0.05\%$ and $S = 0.23 \pm 0.05\%$, and in view of the monomer ratio of 1 to 1 to 8 for C_{11}/PEG/BMA, a DP_n of 27 ± 2 is calculated for the backbone of the terpolymer (eq 1).

$$n = \frac{\%P}{\%S}\frac{(At_w)_S}{(At_w)_P} \quad (1)$$

(52) Senhaji, O.; Robin, J. J.; Achchoubi, M.; Boutevin, B. *Macromol. Chem. Phys.* **2004**, *205*, 1039–1050.

(53) Golander, C. G.; Kiss, E. *J. Colloid Interface Sci.* **1988**, *121*, 240–253.

(54) Matyjaszewski, K.; Davis, T. P. *NetLibrary, I*; Wiley-Interscience: Hoboken, NJ, 2002.

(55) Odian, G. *Principles of Polymerization*, 4th ed.; Wiley: New York, 2004.

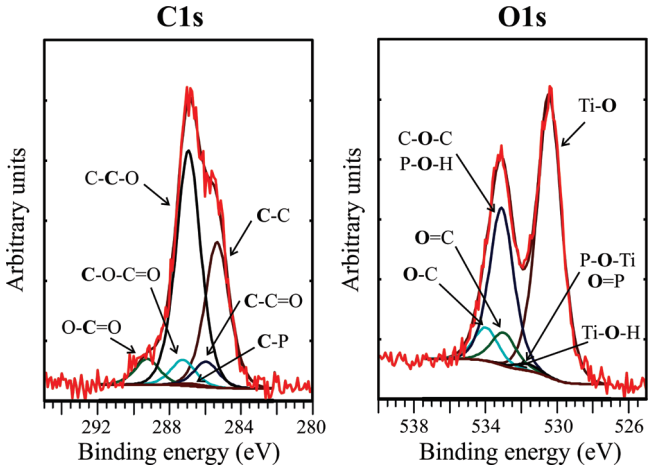

Figure 1. Curve fitted and assigned C 1s and O 1s XPS peaks of the terpolymer adlayer using the fitting parameters of Tables 1 and 2.

This value correlates with the synthesis conditions of initial molar ratio aiming at a DP_n of 30, confirming that chain transfer occurred as polymerization and that the targeted molecular weight was reached.

Terpolymer Assembly on TiO_2. The thickness measured by ellipsometry of the terpolymer adlayer was 30 ± 1 Å.[43] XPS measurements confirmed the adsorption of the phosphorus-PEG-containing polymer on TiO_2: increase of the C 1s intensity and decrease of the Ti 2p intensity in comparison to a bare TiO_2 reference surface as well as by the presence of the P 2p signal.[43] Moreover, strong C−**C**−O and C−**O**−C PEG components were clearly identified in the modeled C 1s and O 1s spectra, respectively (Figure 1).

The determined XPS fitting parameters of the terpolymer system are summarized in Tables 1, 2, and 3. Assuming the average surface stoichiometry of the molecules like in bulk, expected and experimental surface atomic composition of terpolymer coating on TiO_2 matched closely: experimental % (and theoretical %) were found to be 71 ± 1 (72), 28 ± 1 (27.5), and 0.8 ± 0.6 (0.4) for C, O, and P, respectively. Given the theoretical sulfur concentration of 0.1%, XPS was not expected to be sensitive enough to detect S. The very low concentration of phosphorus in the polymer (theoretical value: 0.4%), close to the detection limit of XPS, can explain the statistical deviation (experimental value: 0.8% ± 0.6). Otherwise, as a simplified model, a monodentate binding of the phosphonate groups on TiO_2 was assumed, and component experimental compositions presented in Table 3 confirmed that the polymer structure adsorbed on TiO_2 was similar to that of the bulk polymer.

$$\frac{A_{C-C}}{A_{O-C=O}} = \frac{(N_{C-C})_{Thiol} + \frac{(DP_n)_{backbone}}{1+1/g+r}\left[(N_{C-C})_{C_{11}} + \frac{(N_{C-C})_{PEG}}{g} + (N_{C-C})_{BMA}r\right]}{\frac{(DP_n)_{backbone}}{1+1/g+r}\left[(N_{O-C=O})_{C_{11}} + \frac{(N_{O-C=O})_{PEG}}{g} + (N_{O-C=O})_{BMA}r\right]} \quad (2)$$

$$(DP_n)_{backbone} = \frac{11}{\frac{A_{C-C}}{A_{O-C=O}} - 5.3} \quad (3)$$

A_x is the peak area of the x component with the corresponding specific binding energy, $(N_y)_z$ is the number of y components from the z monomer units, $(DP_n)_{backbone}$ is the number of monomer

Table 3. Theoretical and Experimental Surface Component Composition from C 1s and O 1s Detail Spectra for the Terpolymer Coating Assuming the Average $(DP)_n$ Values of the Adsorbed Molecules Are the Same as in Bulk (Scheme 1) and Using the Fitting Parameters of Tables 1 and 2

components of the terpolymer	theoretical %	experimental %
C−C	31.9	30 ± 1
C−**C**−O−C=O	5.6	5.4 ± 0.2
O−**C**=O	5.6	5.4 ± 0.2
C−C=O	5.6	5.4 ± 0.2
C−**C**−O	50.6	53 ± 1.5
C−P	0.6	0.5 ± 0.1
C−**O**−C=O	15.4	14.2 ± 0.8
O=C	15.4	14.2 ± 0.8
C−**O**−C/P−**O**−H	64.0	62 ± 1.4
P−**O**−Ti/**O**=P	5.0	5.5 ± 0.5

(degree of polymerization in number) of the backbone, $1/g$ is the ratio of PEG/C_{11} monomers, and r is the ratio of BMA/C_{11} monomers.

Additional confirmation that bulk and surface composition match was obtained by determining from the component analysis the different average degrees of polymerization (DP), for the backbone, $(DP_n)_{backbone}$ (eqs 2 and 3) and the PEG chains, $(DP_n)_{PEG}$ (eqs 4, 5, 6, and 7).

$$\frac{A_{C-C-O}}{A_{O-C=O}} = \frac{\frac{(N_{C-C-O})_{PEG}}{g}}{(N_{O-C=O})_{C_{11}} + \frac{(N_{O-C=O})_{BMA}}{g} + (N_{O-C=O})_{PEG}r} \quad (4)$$

$$(DP_n)_{PEG} = 5\frac{A_{C-C-O}}{A_{O-C=O}} \quad (5)$$

$$\frac{A_{C-O-C/P-O-H}}{A_{O-C}} = \frac{\frac{(N_{C-O-C})_{PEG}}{g} + (N_{P-O-H})_{C_{11}}}{(N_{O-C})_{C_{11}} + \frac{(N_{O-C})_{PEG}}{g} + (N_{O-C})_{BMA}r} \quad (6)$$

$$(DP_n)_{PEG} = g\left(10\frac{A_{C-O-C/P-O-H}}{A_{O-C}} - 1\right) \quad (7)$$

The latter can be calculated based on the intensities of the following contributions, C−**C**, O−**C**=O, C−**C**−O, C−**O**−C=O, and C−**O**−C (Table 2), and considering the monomer ratio calculated from ^{1}H NMR. Experimental DP values obtained from analytical characterizations (elemental analysis and SEC) of the bulk terpolymer and calculated DP results using XPS data of the adsorbed terpolymer system on TiO_2 were compared. Experimental DP_n of bulk molecules were determined to be 27 ± 2 (backbone) and 45 ± 1 (PEG) whereas calculated DP_n of adsorbed molecules were 32 ± 3 (backbone) and 49 ± 4 (PEG) using C 1s and O 1s data. We concluded that no selective adsorption from specific fractions of the polydisperse terpolymer solution took place during the assembly and that the polymer layer composition is close to the one of the bulk polymer.

The expected organization in four layers of the monomolecular {terpolymer + substrate} system, schematically drawn in Scheme 1, was compared to the results of the AR-XPS study (Figures 2 and 3). Fitting parameters presented in Tables 1 and 2 were used to plot Figure 3. In Figure 2, ratios are normalized by the highest ratio of the same components within a given series of measurements when varying the angle. C is expected to be a specific element of the top layers (A) and (B), P of the intermediate

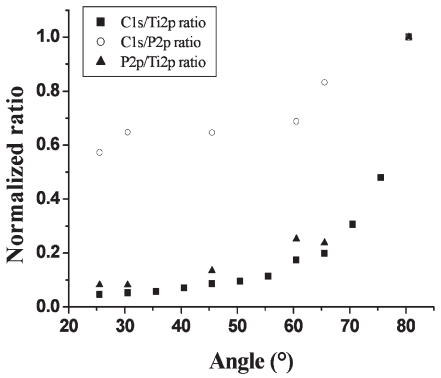

Figure 2. AR-XPS elemental intensity as a function of takeoff angle for the PEG-graft terpolymer adlayer on TiO_2. Ratios of elemental peak areas measured at the same angle were normalized (normalized ratio in the graph) from identical highest ratio obtained within the same series of AR-XPS measurement.

layer (C), and Ti of the substrate layer (D) (Scheme 1). Increase of (C 1s/Ti 2p), (C 1s/P 2p), and (P 2p/Ti 2p) ratios with the takeoff angle confirms the location of the PEG and aliphatic layers (layers A and B, respectively) and P intermediate layer (C) above the TiO_2 substrate (layer D). In Figure 3, {C−**C**−O, C−**O**−C} are expected to be specific components of the PEG layer (A), {**C**−C, O═**C**−O, **C**−**C**−O−C═O, **C**−C═O, **O**═C, O═C−**O**−C} of the intermediate layer (B) containing the backbone and the aliphatic side chains, {**C**−P, **O**═P, P−**O**−Ti} of the anchoring layer (C) with phosphonate groups and Ti−**O** of the substrate (layer D). The insignificant variation of the (O═**C**−O/**C**−C) ratio validates the assumption of backbone and aliphatic side chains being located within the same layer (B), while the increase of the other ratios with takeoff angle confirms the location of the PEG layer at the top (layer A), aliphatic and phosphonate layers (B and C) above the TiO_2 substrate (layer D). "Ratio" is a control value corresponding to the ratio between all C 1s intensities with all O 1s intensities of contributions in layers B and C, including the backbone, the aliphatic side chains, and the phosphonate groups. It must remain more or less constant to be in agreement with the model in Scheme 1. The following tendencies given by normalized ratios with C, P, and Ti atomic intensities were expected, i.e., an increase of detection of both C and P with a decrease of Ti when increasing the takeoff angle of the detector in respect to the surface normal, proving that the C- and P-containing layers are situated above the TiO_2 substrate. Since at the same time the normalized ratio (C 1s/P 2p) increases, the presence of the P-containing intermediate between the TiO_2 layer and the C-containing layer on top is confirmed. The results in Figure 2 corroborated the presence of the organic coating interacting via the phosphonate groups on TiO_2 substrate. The second evaluation (Figure 3) completes the information regarding the internal organization within the polymer coating and especially the location of the PEG chains at the outermost part of the system held below by an aliphatic layer containing the backbone and the anchoring phosphonate side chains. The variations of intensity ratios based on all the characteristic components of each intermediate layer were analyzed in function of the emission angle. Increasing the takeoff angle is expected to result in an increase of the polymer component intensities (**O**═C, C−**O**−C, C−**O**−C═O, **O**═P/P−**O**−Ti) from the aliphatic layers B and C in comparison to titanium oxide contribution (**O**−Ti) in layer D and of the PEG component intensities (C−**C**−O or C−**O**−C) in layer A in comparison to components from the intermediate layers B and C ({**C**−P, O−**C**═O, **C**−**C**−O−C═O, **C**−C═O, **C**−C} and

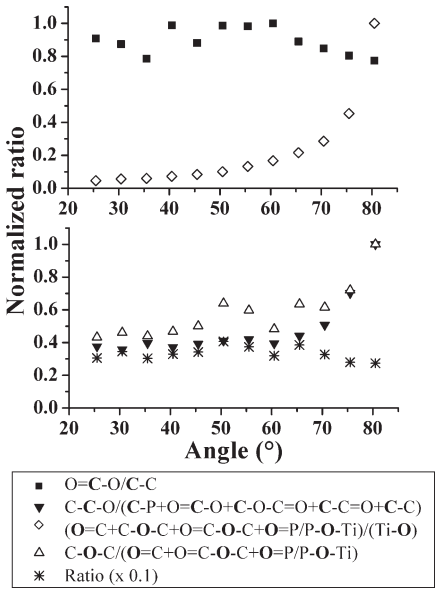

Figure 3. AR-XPS normalized component intensity ratios as a function of takeoff angle for the PEG−poly(phosphonate) terpolymer adlayer on TiO_2. Ratios of component peak areas measured at the same angle were normalized (normalized ratio in the graph) from identical highest ratio obtained within the same series of AR-XPS measurement. "Ratio" is a control value corresponding to the ratio between all C 1s intensities with all O 1s intensities of contributions in layers B and C, including the backbone, the aliphatic side chains, and the phosphonate groups. It must remain more or less constant to be in agreement with the model in Scheme 1.

{**O**═C, C−**O**−C═O, **O**═P/P−**O**−Ti}). Figure 3 presents the ratio evolution as a function of takeoff angle, which correlates with the expectation, i.e., the presence of the PEG layer on the top of the adsorbed organic coating.

In summary, the combined XPS and AR-XPS study in both elements and components proves that the polymer adlayer is characterized by the interaction of phosphonate functions with the TiO_2 substrate and the location of the PEG layer at the outermost surface.

Stability Experiments. The relative changes of the terpolymer adlayer thickness after exposure to different stability test conditions are presented in Figure 4. All results are normalized by the reference value of thickness obtained for the coating right after assembly. To compare the results, two different reference systems that have been extensively described in the literature were chosen. The first one are self-assembled monolayers of dodecylphosphates ($DDPO_4$)[4] used to compare the effect of single versus multiple phosph(on)ate binding groups, and the second system comprises poly(L-lysine)-*grafted*-poly(ethylene glycol) (PLL-*g*-PEG)[25] which assemblies spontaneously from aqueous solution forming monolayers, where the polycationic backbone interacts with negatively charged surfaces by multiple electrostatic interactions. The goal of these tests was to compare the stability of the different coatings in both ionic strength buffers (immersion in 160 mM HEPES solution with pH = 7.4) and at strong pH changes (acidic and basic) (Figure 4).

Stability experiments demonstrate that all three surface coatings were degraded to a higher or lesser degree. The tested media did not lead, however, to the same level of degradation, indicating the strong influence of the nature of the stability test solution. On one hand, after 3 weeks of exposure to low/high pH solutions, the terpolymer layer was not much modified with more than 90%

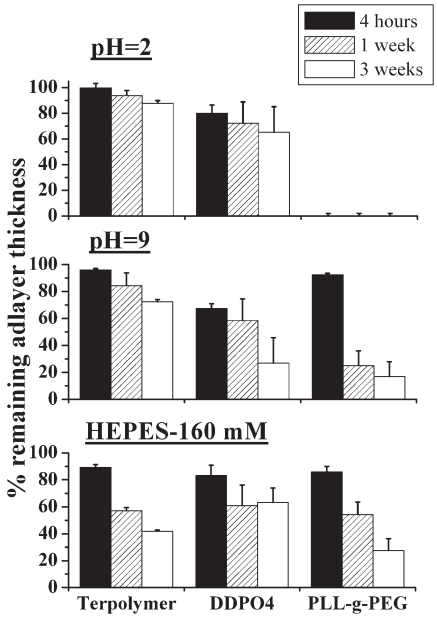

Figure 4. Percentage remaining terpolymer layer thickness on TiO_2 substrate determined by ellipsometry after 4 h, 1 week, and 3 weeks in acidic (pH = 2), basic (pH = 9), and salt (160 mM HEPES, pH = 7.4) solutions at room temperature. For comparisons, two reference systems were included: a SAM of dodecylphosphate ($DDPO_4$)[4] and a PLL-*g*-PEG copolymer adlayer, both on TiO_2 surfaces.[25]

remaining thickness at pH = 2 and more than 70% at pH = 9, in comparison to the reference systems that generally degraded to a much higher extent (60% maximum thickness remaining for the best results). On the other hand, the test at increased ionic strength of 160 mM and duration of 3 weeks led to a strong covering adlayer thickness reduction with less than 50% remaining thickness. In comparison to the two reference systems, $DDPO_4$ and PLL-*g*-PEG, the overall stability of the terpolymer adlayer on TiO_2 in the different media is largely improved. The origin of such improved stability properties shown with this matrix of experiments is believed to reside in the combination of the cooperative multisite attachment and the strong coordination of the phosphonate groups to the TiO_2 substrate provided by the polymer structure.

Concerning the decrease of poly(phosphonate) adlayer thickness (Figure 4) during stability tests, complementary XPS information presented in Figure 5 allowed us to draw some conclusions regarding the mechanism of degradation. First, the XPS (C 1s/Ti 2p) atomic ratio decreased with time of exposure to solutions confirming the loss of polymeric material from the surface. Second, it was noticed that both (**C**−C/Ti 2p) and (C−**C**−O/Ti 2p) normalized intensity ratios specific to the PEG layer (A) and aliphatic layer (B), respectively (Scheme 1), showed a different dependence on exposure time to the stability solutions as presented in Figure 6. Moreover, the degradation depended on whether the surfaces were stored in the presence or absence of (laboratory) light. The loss of PEG was more substantial in comparison to the aliphatic parts of the coating.

The different degradation behavior indicated by the (**C**−C/Ti 2p) aliphatic and (C−**C**−O/Ti 2p) PEG intensity ratios suggests that the polymer does not simply desorb from the surface but that rather a PEG-specific degradation process took place. This is also supported by the P surface concentration that slightly increased than decreased with exposure time (0.9% ± 0.5, 1.4 ± 0.7, and 1.5% ± 0.5 for pH = 2, pH = 9, and 160 mM HEPES, respectively) in

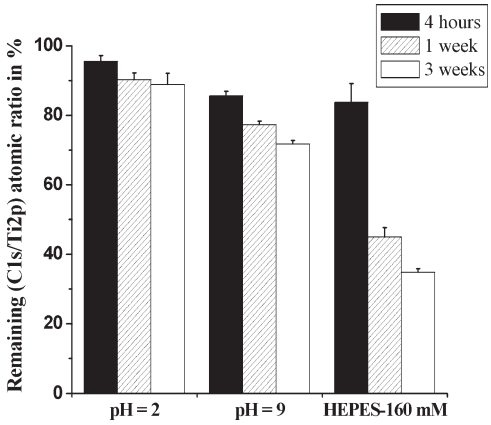

Figure 5. Percentage remaining C 1s/Ti 2p atomic ratios for the terpolymer adlayer system measured by XPS on TiO_2 after 4 h, 1 week, and 3 weeks in acidic (pH = 2), basic (pH = 9), and salt (160 mM HEPES) solutions at room temperature in comparison to the C 1s/Ti 2p ratios before exposure to the different media.

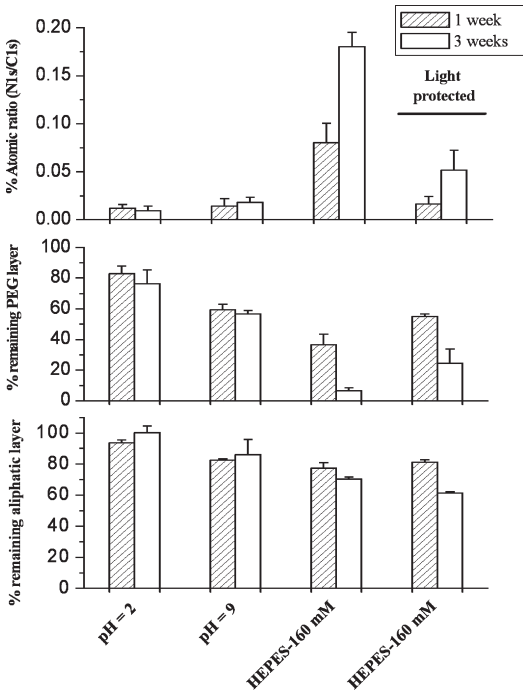

Figure 6. Percent remaining aliphatic and PEG layers of terpolymer coatings on TiO_2 judged by the XPS (**C**−C/Ti 2p) and (**C**−C−O/Ti 2p) intensity ratios after 1 and 3 weeks exposure to pH 2, pH 9, and HEPES 160 mM (pH 7.4, with and without light exposure) compared to the corresponding values before exposure to the test solutions. The degree of serum protein adsorption (15 min) to the polymer-coated and 1/3 weeks solution-exposed surfaces was judged by the XPS atomic ratio (N 1s/C 1s).[43,53] For comparison, the (N 1s/C 1s) atomic ratio of a bare titania substrate exposed to serum is about 0.225 ± 0.006.

comparison to the adlayer right after assembly (0.8% ± 0.2). One possible explanation for the PEG degradation process could be the hydrolysis of the ester functions between side chains and backbone (Scheme 1), mechanism favored either by extreme pH conditions and/or the increasing ionic strength of solution.[56] This seems not to be the case, since (1) no reduction in both XPS component

(56) Makino, K.; Ohshima, H.; Kondo, T. *J. Microencapsulation* **1986**, *3*, 203–212.

C−**C**−O−C═O and C−**O**−C═O intensities corresponding to the ester function has been noticed when analyzing samples exposed to all stability solutions, (2) all the tests performed under harsh conditions in pH, i.e., pH = 2 and 9, did result in less PEG reduction in comparison to 160 mM HEPES buffer at pH 7.4 (Figure 6), and (3) a sample exposed to ultrapure water for 3 weeks showed less remaining adlayer and PEG content than in contact to a 10 mM HCl solution, i.e., at pH = 2, for the same period (76.9 ± 1% and 66.7 ± 0.1% versus 90.3 ± 2% and 76.3 ± 9.2%, respectively).

Given the above observations and the additional effect of light, the mechanism responsible for the PEG modifications is believed to originate from an internal degradation such as autoxidation. According to the literature, PEG autoxidizes in the solid state,[57] in diluted solutions,[58] and in surface-immobilized state,[59−62] modifying its protein-resistant properties at long-term under in vivo conditions.[61,63] In light of previous references describing the variations of PEG systems exposed to aqueous and biological solutions at both short and long term, it is therefore legitimate to assume that PEG autoxidation is also effective in 160 mM HEPES solution. Initiation of the process happens by the formation of peroxides,[58,64] mediated by free-radical sources,[58] or photochemical reactions by exposure to near-UV light.[58,65] However, degradation has been reported to be still substantial in the dark, albeit at lower rates compared to free-radical initiation or UV exposure.[58,66,67]

Variation of the pH in both acid and basic directions has been proven to have no strong influence on the autoxidation kinetic,[68] which is in agreement with our experimental results when comparing tests in pH = 2 and 9 solutions with 160 mM HEPES buffer at pH = 7.4 with the latter showing lower remaining PEG amounts (Figure 6). Finally, the suggestion of an autoxidation mechanism is supported by the results showing the dependence of light exposure on the PEG layer degradation for samples immersed in 160 mM HEPES. Samples were exposed to test solutions in polystyrene plastic cell plates that transmit UV-A and partly UV-B radiations[69] while reference measurements were performed in solutions protected by an aluminum foil. The strong degradation of the PEG layer when not protected to light attributed to near-UV-initiated oxidation[58,65] match with the autoxidation mechanism described in the literature. It is also supported later by the results of Figure 7, with the series of experiments using Nb_2O_5 surfaces.

The variations observed in the aliphatic and PEG layer degradation (Figure 6) suggest that another mechanism, related to the substrate (TiO_2) properties, is acting in addition to PEG autoxidation. To prove this hypothesis, assemblies and stability tests in the most degrading solution, i.e., 160 mM HEPES, and in the presence and absence of light were performed using a second type of claimed inert substrate: Nb_2O_5. Corresponding XPS results are shown in Figure 7.

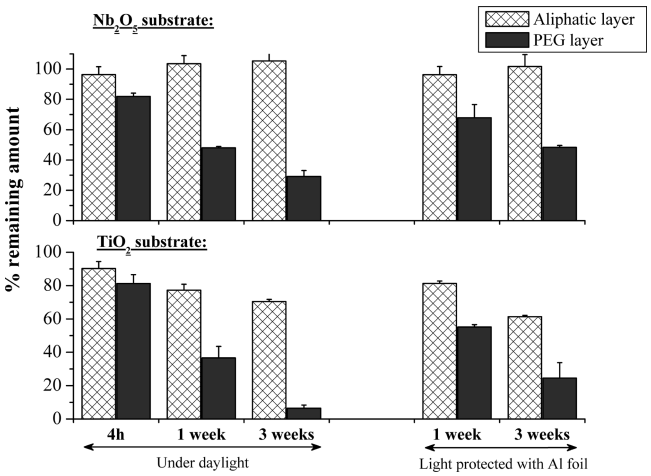

Figure 7. Percent remaining aliphatic and PEG layers of the terpolymer-coated TiO_2 and Nb_2O_5 substrates (judged by the XPS **C**−C/Ti 2p and **C**−C−O/Ti 2p intensity ratios) in comparison to the corresponding values before exposure to the test solutions. Samples were immersed in 160 mM HEPES buffer (pH = 7.4) for 4 h, 1 and 3 weeks at room temperature, with and without exposure of the samples to light during the tests.

In the case of Nb_2O_5 substrate, the aliphatic layer remains almost constant all along the stability tests in 160 mM HEPES buffer, while the PEG layer is still degrading. However, in comparison to the results with TiO_2 surfaces, more PEG material is remaining. Like in the case of TiO_2, the exposure to light is also influencing the progress of PEG degradation.

First of all, results obtained on inert Nb_2O_5 surfaces confirm the PEG autoxidation of the adsorbed terpolymer molecules on TiO_2 in contact at the interface to aqueous solutions and the kinetic dependence of the PEG degradation with exposure to daylight. Second, as suggested by the results in Figures 6 and 7, an additional process of adlayer instability to PEG autoxidation is occurring which we attribute to the known photochemical activity of titania substrate.

TiO_2 is a material of importance in solar energy conversion,[70−72] sunscreens,[73,74] and organic decontamination of sewage waters.[71,75−77] Indeed, titania illuminated with UV-B (290−320 nm) and part of UV-A (320−400 nm) can generate electron−hole pairs on its surface, producing subsequently from adsorbed O_2, H_2O, or organic contaminants highly reactive oxygen species which degrade organic material through catalytic reactions.[78−80] Consequently, ordinary room light is sufficient to

(57) Han, S.; Kim, C.; Kwon, D. *Polym. Degrad. Stab.* **1995**, *47*, 203–208.
(58) Donbrow, M. *Nonionic Surfactants: Phys. Chem.* **1987**, *23*, 1011–1073.
(59) Branch, D. W.; Wheeler, B. C.; Brewer, G. J.; Leckband, D. E. *Biomaterials* **2001**, *22*, 1035–1047.
(60) Sharma, S.; Johnson, R. W.; Desai, T. A. *Langmuir* **2004**, *20*, 348–356.
(61) Zhang, F.; Kang, E. T.; Neoh, K. G.; Wang, P.; Tan, K. L. *J. Biomed. Mater. Res.* **2001**, *56*, 324–332.
(62) Bindra, D. S.; Williams, T. D.; Stella, V. J. *Pharm. Res.* **1994**, *11*, 1060–1064.
(63) Fan, X. W.; Lin, L. J.; Messersmith, P. B. *Biomacromolecules* **2006**, *7*, 2443–2448.
(64) Yang, L.; Heatley, F.; Blease, T. G.; Thompson, R. I. G. *Eur. Polym. J.* **1996**, *32*, 535–547.
(65) Montague, M.; Ducker, R. E.; Chong, K. S. L.; Manning, R. J.; Rutten, F. J. M.; Davies, M. C.; Leggett, G. J. *Langmuir* **2007**, *23*, 7328–7337.
(66) Bergh, M.; Magnusson, K.; Nilsson, J. L. G.; Karlberg, A. T. *Contact Dermatitis* **1998**, *39*, 14–20.
(67) Bergh, M.; Shao, L. P.; Hagelthorn, G.; Gafvert, E.; Nilsson, J. L. G.; Karlberg, A. T. *J. Pharm. Sci.* **1998**, *87*, 276–282.
(68) Crouzet, C.; Decker, C.; Marchal, J. *Makromol. Chem., Macromol. Chem. Phys.* **1976**, *177*, 145–157.
(69) Xue, Y. M.; Nicholson, W. L. *Appl. Environ. Microbiol.* **1996**, *62*, 2221–2227.
(70) Hsiao, P.-T.; Wang, K.-P.; Cheng, C.-W.; Teng, H. *J. Photochem. Photobiol., A* **2007**, *188*, 19–24.
(71) Orendorz, A.; Brodyanski, A.; Losch, J.; Bai, L. H.; Chen, Z. H.; Le, Y. K.; Ziegler, C.; Gnaser, H. *Surf. Sci.* **2007**, *601*, 4390–4394.
(72) Fujishima, A.; Rao, T. N.; Tryk, D. A. *J. Photochem. Photobiol., C* **2000**, *1*, 1–21.
(73) Konaka, R.; Kasahara, E.; Dunlap, W. C.; Yamamoto, Y.; Chien, K. C.; Inoue, M. *Redox Report* **2001**, *6*, 319–325.
(74) Siddiquey, I. A.; Ukaji, E.; Furusawa, T.; Sato, M.; Suzuki, N. *Mater. Chem. Phys.* **2007**, *105*, 162–168.
(75) Tayade, R. J.; Surolia, P. K.; Kulkarni, R. G.; Jasra, R. V. *Sci. Technol. Adv. Mater.* **2007**, *8*, 455–462.
(76) Hoffmann, M. R.; Martin, S. T.; Choi, W. Y.; Bahnemann, D. W. *Chem. Rev.* **1995**, *95*, 69–96.
(77) Carp, O.; Huisman, C. L.; Reller, A. *Prog. Solid State Chem.* **2004**, *32*, 33–177.
(78) Kanta, A.; Sedev, R.; Ralston, J. *Langmuir* **2005**, *21*, 2400–2407.
(79) Lee, J. P.; Kim, H. K.; Park, C. R.; Park, G.; Kwak, H. T.; Koo, S. M.; Sung, M. M. *J. Phys. Chem. B* **2003**, *107*, 8997–9002.
(80) Takeuchi, M.; Martra, G.; Coluccia, S.; Anpo, M. *J. Phys. Chem. C* **2007**, *111*, 9811–9817.

initiate such a process.[72,81−83] However and surprisingly, it has been published that TiO_2 surfaces in complete dark can also initiate photo-"like" reduction of O_2.[72]

Consequently, we attribute part of the observed additional degradations affecting both aliphatic and PEG layers (Figures 6 and 7) to reactive species generated by TiO_2 under both light and dark conditions. The extension of the degradation to the whole adlayer is due to surface migration and diffusion ability through the terpolymer adlayer of the created active units.[79,84,85] In view of the higher adlayer degree of (both aliphatic and PEG) degradation observed for the tests in 160 mM HEPES buffer (in comparison to low/high pH solutions), we assume that either the TiO_2-related substrate photocatalytic degradation activity is enhanced by the HEPES buffer components or alternatively that the higher ionic strength of the 160 mM HEPES buffer enhances the degradation; the latter mechanism is supported by the observation that with increasing ionic strength the activation energies of TiO_2 photoreactions usually decrease.[86] Complementary experiments are required to determine precisely the specific roles of HEPES molecules and/or ionic strength on the photocatalytic mechanism.

Finally, the active role of the titania substrate in the polymer degradation is confirmed when comparing the latter to the results of the experiments on the Nb_2O_5 surface, which is known to have less photocatalytic activity[87] and exhibits significantly reduced degradation in comparison to TiO_2 (Figure 7).

Resistance of the Adlayer against Protein Adhesion. A preliminary study using ex situ ellipsometry and XPS has already shown that the poly(phosphonates) PEG−terpolymer interface has nonfouling properties (exposure for 4 h in 160 mM HEPES buffer followed by 15 min full human serum exposure).[43]

Here we used the in situ, quantitative OWLS technique to quantitatively prove the reported resistance ability of the terpolymer adlayer to protein adsorption. The corresponding adsorbed serum mass was found to be 4 ± 1 ng/cm^2, which corresponds to a reduction by 98% in comparison to bare TiO_2 (150−250 ng/cm^2 [7]). Second, in view of previous results proving the variations in the terpolymer adlayer and especially of its PEG layer during long time exposure to electrolyte solutions, changes were expected in the remaining of the nonfouling property initially imparted to TiO_2 surfaces. Consequently, protein adsorption experiments were performed on samples resulting right after stability tests, following the standard protocol described previously. XPS was used as characterization technique to evaluate the degree of protein adsorption, especially by calculating the atomic ratio (N 1s/C 1s) with XPS data.[43,53] Figure 6 summarizes the (N 1s/C 1s) ratios obtained after serum exposure of the stability test samples in combination to the percentage of remaining PEG layer information. A direct consequence of the terpolymer coating degradation during long-term stability tests, and especially of the PEG layer, is an alteration of the nonfouling property as shown in Figure 6. Indeed, a decrease of the amount of PEG correlates with an increase in the adsorption of proteins characterized by higher atomic ratio (N 1s/C 1s) values. In comparison to previously published conclusions with freshly assembled terpolymer adlayers exposed directly to serum,[43] the results obtained after 3 weeks of exposure at pH = 2 suggest that the nonfouling property is remaining all along effective as long as 80% PEG layer (atomic composition) remains. Finally, it should be mentioned that even in the worst case, i.e., using the samples exposed for 3 weeks to 160 mM HEPES, resulting in the most advanced PEG decrease, the amount of adsorbed proteins was still lower than a full protein layer covering a bare TiO_2 substrate (see Figure 6).

Conclusions

Poly(phosphonates) PEG−terpolymer molecules self-assembled according to an organized scheme characterized by the binding of phosphonate groups to TiO_2 substrate and the formation of a PEG−brush layer at the outermost surface of the coating. In comparison to reference systems (SAMs and polyelectrolyte-grafted polymer adlayers), this new terpolymer interface was able to present overall stability improvements against desorption in contact with aqueous solutions. Nevertheless, the long-term stability at room temperature was hampered by two degradation mechanisms: photocatalytic activity of titania substrate and autoxidation of PEG, both of which affected the kinetics of polymer adlayer. However, the origin(s) and precise mechanism(s) of these adlayer changes that depend on the type of aqueous media, in particular type and ionic strength of the salt solution, remain largely unknown and require further investigations.

Beside the stability performance, the PEG−terpolymer adlayer proved to impart to the TiO_2 substrate antifouling properties at short term and under biologically relevant conditions (i.e., 2% protein uptake upon serum exposure in comparison to a bare TiO_2 surface). After longer time exposure to electrolyte solutions, the persistence of the protein resistance was shown to remain as long as the degree of PEG layer degradation was less than 20%.

On the basis of the insight gained in this work regarding the factors that affect degradation, we suggest replacing PEG by suitable alternatives such as polyoxazolines[88] or using different substrate treatments[89,90] with the aim of producing stable and reusable chips presenting nonfouling backgrounds. Moreover, functionalization of the poly(phosphonate) terpolymer structure with specific bioligands/carriers/spacers would open potential applications, in particular in the field of biosensors.[91]

Acknowledgment. The authors are grateful to ETH Zurich (Project TH-25/03-2), Swiss National Science Foundation (SNF, Grant 200021-112266), and Université de Montpellier II for financial support. Grégory Foulonneau, Audrey Quinqueneau, Sophie Martin, Geoffroy Leveque, Julien Zugmeyer, François Picon and Sabrina Bozzini are thanked for their contributions and support with the synthesis, characterization of the polymers and preliminary surface modifications.

(81) Kanta, A.; Sedev, R.; Ralston, J. *Colloids Surf., A* **2006**, *291*, 51–58.
(82) Kavitha, R.; Meghani, S.; Jayaram, V. *Mater. Sci. Eng., B* **2007**, *139*, 134–140.
(83) Wan, L.; Li, J. F.; Feng, J. Y.; Sun, W.; Mao, Z. Q. *Mater. Sci. Eng., B* **2007**, *139*, 216–220.
(84) Haick, H.; Paz, Y. *J. Phys. Chem. B* **2001**, *105*, 3045–3051.
(85) Murakami, Y.; Endo, K.; Ohta, I.; Nosaka, A. Y.; Nosaka, Y. *J. Phys. Chem. C* **2007**, *111*, 11339–11346.
(86) Kozlov, D. V.; Panchenko, A. A.; Bavykin, D. V.; Savinov, E. N.; Smirniotis, P. G. *Russ. Chem. Bull.* **2003**, *52*, 1100–1105.
(87) A. Oliveira, L. C.; Ramalho, T. C.; Goncalves, M.; Cereda, F.; Carvalho, K. T.; Nazzarro, M. S.; Sapag, K. *Chem. Phys. Lett.* **2007**, *446*, 133–137.
(88) Konradi, R.; Pidhatika, B.; Muhlebach, A.; Textor, M. *Langmuir* **2008**, *24*, 613–616.
(89) Egerton, T. A.; Everall, N. J.; Mattinson, J. A.; Kessell, L. M.; Tooley, I. R. *J. Photochem. Photobiol., A* **2007**, *193*, 10–17.
(90) Xie, T.-H.; Lin, J. *J. Phys. Chem. C* **2007**, *111*, 9968–9974.
(91) Davies, R. C.; Neuberge, A.; Wilson, B. M. *Biochim. Biophys. Acta* **1969**, *178*, 294–305.